Research on the Vibration Characteristics of Rolling Bearing Based on ANSYS Software

Yongmei Wang[1,*], Changwei Miao[2], Xiaodong Zhou[2]
[1]School of Physics and Telecommunication Engineering, Zhoukou Normal University, Zhoukou, Henan, China
[2]School of Mechanical and Electrical Engineering, Zhoukou Normal University, Zhoukou, Henan, China
**Corresponding Author*

Abstract: Rolling bearings are a key component in the operation of numerical control machine tool, directly affecting the reliability and safety of the entire equipment. With the rapid development of industrialization in our country, high-performance rolling bearings are becoming urgently needed products in the field of industrial manufacturing, and the study of vibration characteristics is related to the quality issues and safety performance of the bearings. This paper takes deep groove ball bearing SKF6180 as an example to conduct modal and forced excitation vibration analysis of rolling bearings. The natural frequencies of the rolling bearings under free and constrained conditions are obtained. Harmonic response vibration analysis of the bearing is carried out to obtain the frequency amplitude curve of the bearing under external excitation load, providing a theoretical foundation for improving the service life of bearings and the stability of mechanical structures.

Keywords: Rolling Bearing; Finite Element Method; Modal Analysis; Vibration Characteristics.

1. Introduction

Rolling bearings are crucial support components widely used in rotary machinery. Once a fault occurs, it may affect the normal operation of the entire equipment, causing significant economic losses. During the long service life of rolling bearings, various localized faults such as indentations, spalling, wear, and pitting may appear. Conducting dynamic modeling and vibration analysis of rolling bearings with localized faults has important theoretical value and engineering significance, thus attracting extensive attention from scholars both domestically and internationally.

In recent years, many scholars have studied the dynamic characteristics of defective rolling bearings. Liu et al.[1-2] summarized the features of local and distributed defects in rolling bearings and reviewed the fault diagnosis of cylindrical roller bearings considering both local and distributed defects, pointing out the challenges, directions, and impacts in dynamic modeling and analysis methods for local and distributed faults. He et al. [3-6] established the dynamics model of cylindrical roller bearings with local defects and conducted simulation analyses on the vibration responses of single-defect, multi-defect, and compound-fault bearings, proposing a numerical noise hypothesis to estimate noise frequencies. Ma Hui et al. [7-10] established finite element simulation models for typical faults such as inner ring and outer ring, analyzing the equivalent stress in the fault area and the process of rollers passing over local defects through cloud diagrams; they used envelope spectrum transformation to identify fault characteristic frequencies from extracted node acceleration, velocity, and displacement signals.

This paper uses the ANSYS finite element analysis software, taking deep groove ball bearing SKF6180 as the research object, and uses Pro/E three-dimensional modeling software for three-dimensional modeling of rolling bearings. The model is imported into ANSYS, and based on meshing, loading, and boundary constraints, modal and harmonic response finite element analyses of the rolling bearing are conducted to obtain relevant vibration characteristics of the rolling bearing, which can provide certain reference for

structural optimization of the bearing.

2. 3D Modeling of Rolling Bearing

The greatest advantage of the 3D modeling software Pro/E is its ability to perform parametric settings, using a single database for management. By changing parameters in an individual structure through correlation, corresponding module changes can be achieved in the 3D model. Pro/E has distinct modeling features, well-organized modules, and powerful surface modeling capabilities. It supports operations such as sketching, part creation, assembly, and motion simulation, meeting various modeling needs of users. It is widely used in mechanical design, mold development, aerospace, and other fields. Considering the structural composition of rolling bearings, outline sketches are drawn, extruded into shape, and then different planes are established as references. Using various modeling features of Pro/E, the local features of rolling bearings are gradually constructed, as shown in **Figure 1**.

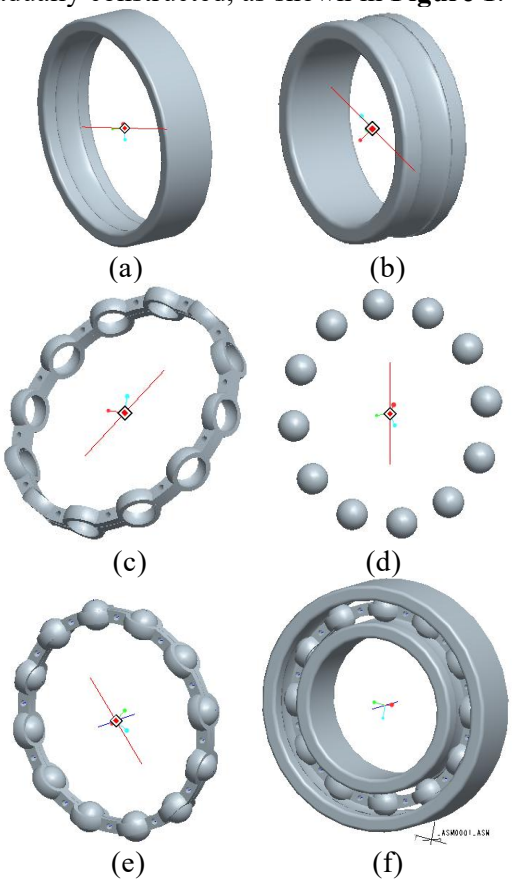

Figure 1. 3D Model of Rolling Bearing, (a) Rolling bearing outer ring; (b) Rolling bearing inner ring; (c) rolling bearing cage; (d) rolling bearing balls; (e) rolling bearing cage and balls; (f) Rolling bearing model.

3. Modal Analysis of Rolling Bearings

3.1 Free Modal Analysis of Rolling Bearings

Modal analysis is the foundation for studying structural vibrations and serves as the basis for describing the dynamic characteristics of mechanisms [11-12]. Using ANSYS for modal analysis of rolling bearings can yield relevant modal parameters, laying the groundwork for research on the vibration response of rolling bearings. The free modal frequencies of the rolling bearings obtained from simulation are shown in **Figure 2**.

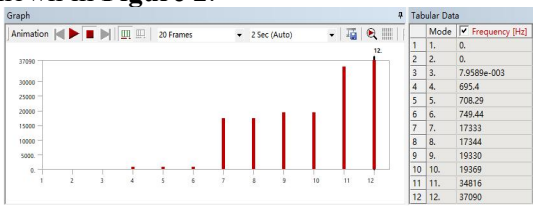

Figure 2. Free Mode Frequency Spectrum Diagram of Rolling Bearing

From the modal spectrum diagram (**Figure 2**), it can be seen that the first three natural frequencies of the deep groove ball bearing are almost zero, while the fourth to sixth natural frequencies are not zero but very weak compared to the bearing vibration frequency. The results indicate that in the free modal state, the first six orders of the rolling bearing are rigid body vibrations, and the rolling bearing does not produce vibration deformation. As the modal order increases, the natural frequency will increase at different speeds; from the seventh to tenth order, the frequency growth is relatively gentle, while the eleventh and twelfth orders grow faster.

The deformations of the rolling bearing at the 7th, 9th, 11th, and 12th modal orders are shown in **Figures 3, 4, 5 and 6**. The 7th order mode shape shows the upper and lower parts of the outer ring of the rolling bearing bending inward. In the 9th order mode, the rolling bearing undergoes an overall compression deformation into an elliptical shape. The 11th order mode shape indicates that the inner ring of the bearing deforms outward. The 12th order mode shape of the rolling bearing involves a torsional deformation at a certain angle on the inner circular ring.

3.2 Constrained Mode of Rolling Bearing

The modal characteristics of a rolling bearing structure are related to its shape, material, and

constraints. Compared to free modes, modal analysis under constrained conditions better reflects the actual operating state of the bearing. In practical operation, there are two types of constraint scenarios for rolling bearings: the first type involves the outer ring being fixed while the inner ring rotates with the balls; the second type involves the inner ring being fixed while the outer ring rotates with the balls.

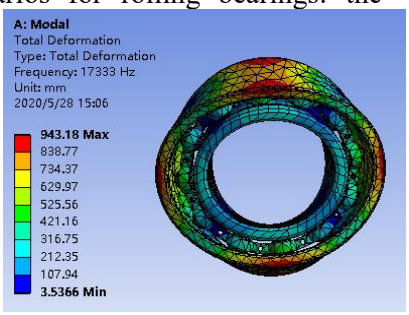

Figure 3. 7 Order Free Mode

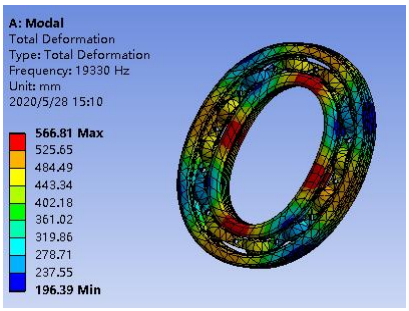

Figure 4. 9 Order Free Mode

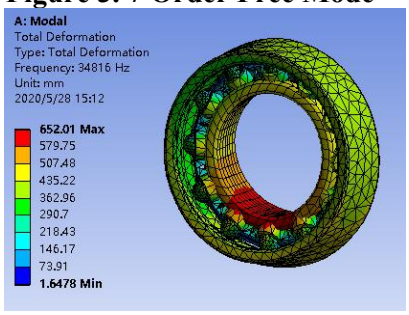

Figure 5. 11 Order Free Mode

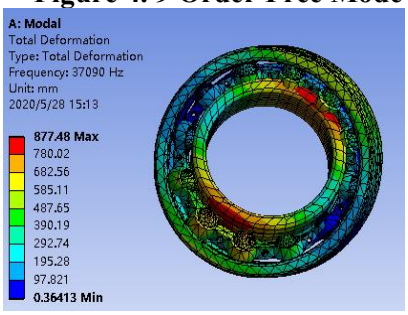

Figure 6. 12 Order Free Mode

3.2.1 The first type of constraint modal for rolling bearings: Outer ring fixed

When the outer ring of deep groove rolling bearing is restrained, the mode frequencies of rolling bearing under constrained conditions from 1 order to 6 order are shown in **Figure 7**.

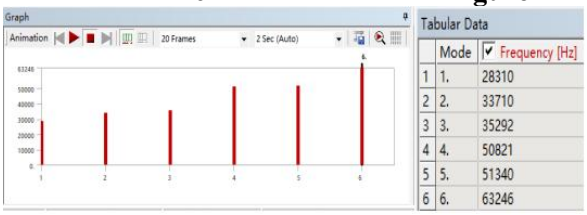

Figure 7. Constrained Modal Frequency of Rolling Bearing(Outer Ring Fixed)

The constrained modal analysis from 1 order to 4 order were carried out as shown in Figures 8, 9, 10 and 11. By examining the cloud diagrams from the 1st to the 4th order, it can be observed that the vibration mode of the 1st constrained modal of the rolling bearing shows an outward protruding deformation of the inner ring at the center, with the balls also protruding outward, as shown in **Figure 8**. In **Figure 9**, the 2nd order mode shows a certain angle deflection bending of the inner ring of the rolling bearing, and the cage undergoes compressive deformation. The 3rd order mode shows an upward and downward tensile deflection displacement on both sides of the bearing's inner ring, as shown in **Figure 10**. The 4th order constrained modal of the bearing shows an inward bending deformation on the upper and lower sides of the inner ring, with tensile deformation appearing on the left and right sides, and the cage undergoing torsional deformation, as shown in **Figure 11**.

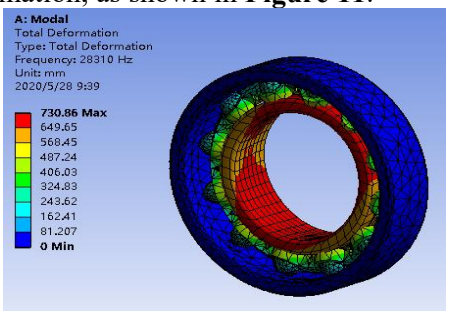

Figure 8. 1 Order Constrained Mode under the Outer Ring Being Restrained

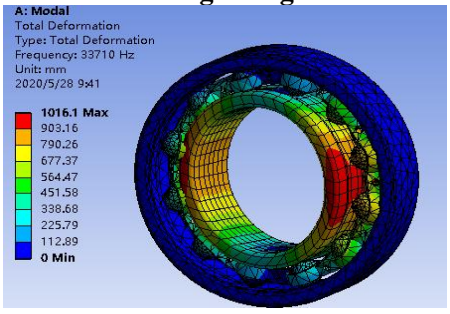

Figure 9. 2 Order Constrained Mode under the Outer Ring Being Restrained

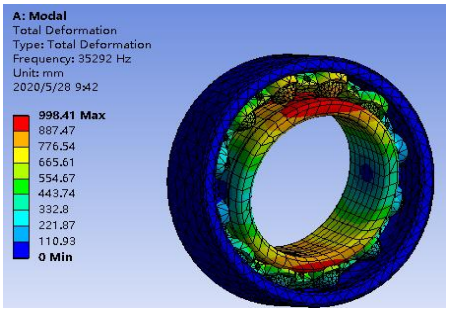

Figure 10. 3 Order Constrained Mode under the Outer Ring Being Restrained

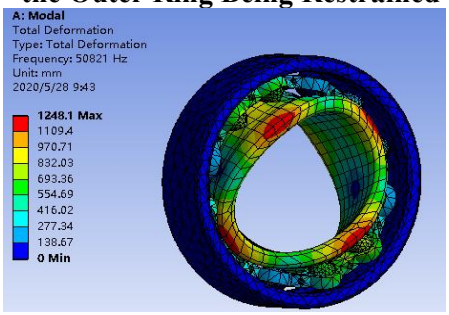

Figure 11. 4 Order Constrained Mode under the Outer Ring Being Restrained

3.2.2 The second type of constraint modal for rolling bearings: inner ring fixed

When the inner ring of deep groove rolling bearing is restrained, the mode frequencies of rolling bearing under constrained conditions from 1 order to 8 order are shown in **Figure 12**. And the constrained modal analysis from 1 order to 4 order were also carried out as shown in **Figures 13, 14, 15, and 16**.

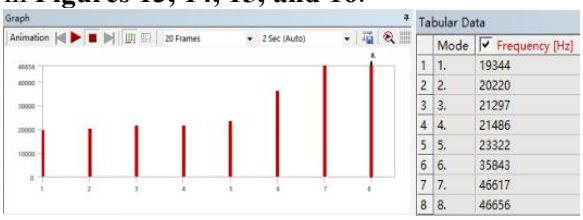

Figure 12. Constrained Modal Frequency of Rolling Bearing(Inner Ring Fixed)

Combining the comprehensive modal deformation and the frequency diagrams of each order of modal frequencies, by examining the constrained mode cloud diagrams from the 1 , 3, 5, and 7 order, it can be observed that the 1 order mode shape involves an outward twisting deformation on one side of the outer ring of the rolling bearing, which also causes the cage to undergo a tilting displacement (**Figure 13**). The 3 order mode deformation of the rolling bearing involves bending deformations on both sides of the outer ring and the cage (**Figure 14**). The 5 order constrained mode shape shows a bending deformation at a certain angle towards the inside on one side of the bearing's outer ring (**Figure 15**). The 7 order mode shape exhibits a triangular twisting deformation on both sides of the bearing's outer ring (**Figure 16**).

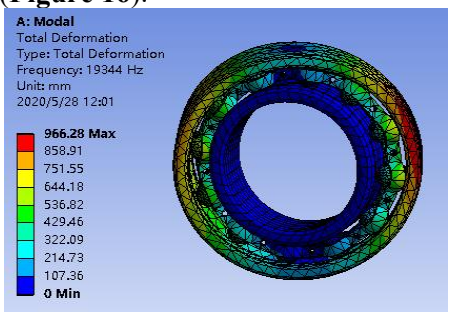

Figure 13. 1 Order Constrained Mode under the Inner Ring Being Restrained

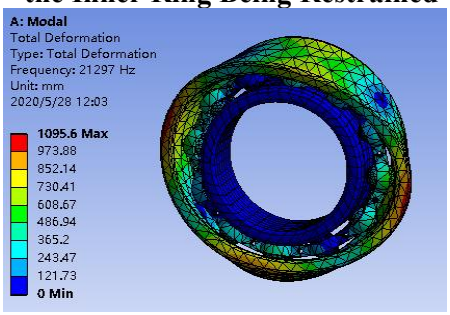

Figure 14. 3 Order Constrained Mode under the Inner Ring Being Restrained

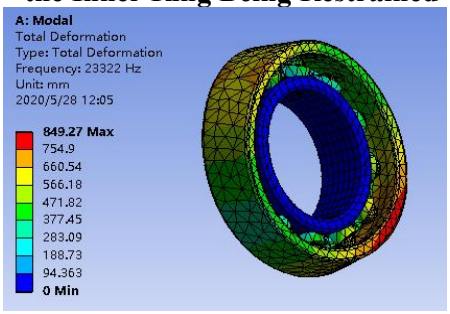

Figure 15. 5 Order Constrained Mode under the Inner Ring Being Restrained

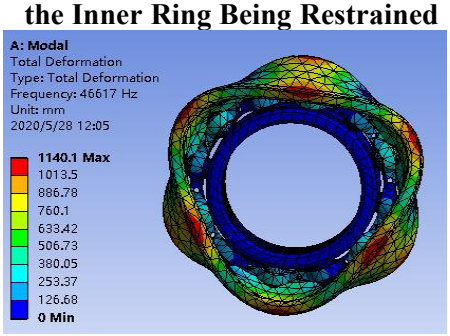

Figure 16. 7 Order Constrained Mode under the Inner Ring Being Restrained

From the modal shapes under two types of constraint conditions, it can be observed that: for the first type of constraint modal shape, the vibration deformation mainly occurs on the inner ring and the cage, with the maximum deformation area located at the edge of the inner ring raceway; for the second type of constraint modal shape, it is exactly the opposite,

where the outer ring and the cage exhibit significant vibration deformation, with the maximum deformation area located at the edge of the outer ring raceway. When the external excitation frequency approaches the natural frequency, this mode of the bearing may be activated, leading to severe vibrations, which could result in the fracture of the inner and outer rings in severe cases. This structural damage caused by resonance effects is detrimental to the stable operation and safe production of rotary machinery.

4. Harmonic Response Analysis of Rolling Bearing

The harmonic response analysis based on ANSYS software includes three methods: complete method, modal superposition method and reduction matrix method [13, 14]. In this paper, the vibration response of rolling bearing is studied based on modal superposition method. The forced vibration response curves of the inner ring of rolling bearing were obtained by applying sinusoidal excitation load to the inner ring ring of rolling bearing.

The frequency vibration displacement curve of the rolling bearing in the X direction is shown in **Figure 17**. By observation, it can be seen that the initial vibration frequency of the rolling bearing is 833.33 Hz, with a vibration displacement of 2.03×10^{-4} mm. From 833.33 Hz to 27500 Hz, the amplitude change of the rolling bearing in the X direction is small. At 28333 Hz, an amplitude peak of 0.134 mm appears, which is near the first natural frequency of the rolling bearing at 28310 Hz, making resonance highly likely. When the rolling bearing operates between 28333 Hz - 50000 Hz, the vibration displacement decreases to 1.23×10^{-4} mm.

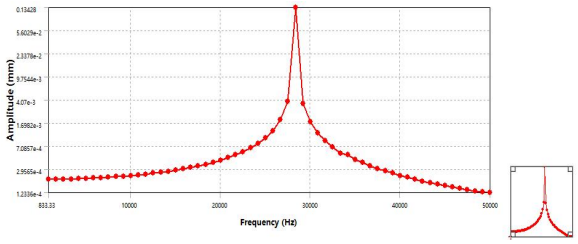

Figure 17. Rolling Bearing Amplitude Curve in the X Direction

The frequency vibration displacement curve of the rolling bearing in the Y direction is shown in **Figure 18**. By observation, it can be seen that at the initial frequency of 833.33 Hz, the vibration displacement of the rolling bearing is 1.18×10^{-3} mm. Within the range of 833.33 Hz to 27500 Hz, the displacement of the rolling bearing does not change much, and the amplitude value is relatively small. At a frequency of 28333 Hz, the displacement of the rolling bearing reaches its peak of 0.19 mm. Between 28333 Hz and 34167 Hz, the amplitude gradually decreases to 7.34×10^{-6} mm. From 34167 Hz to 50000 Hz, the displacement of the rolling bearing in the Y direction gradually increases to 9.06×10^{-4} mm.

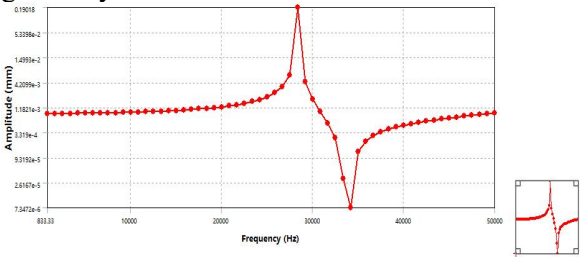

Figure 18. Rolling Bearing Amplitude Curve in the Y Direction

The frequency vibration displacement curve of the rolling bearing in the Z direction is shown in **Figure 19**. By observation, it can be seen that the initial vibration frequency of the rolling bearing in the Z direction is 833.33 Hz, with an amplitude of 1.106×10^{-3} mm, and maintains this amplitude value over a longer frequency range without change until it reaches 26667 Hz, at which point it decreases to 2.27×10^{-4} mm. Between 26667 Hz and 28333 Hz, the amplitude rapidly rises to 0.085 mm. Then, in subsequent frequency ranges, it basically maintains around an amplitude value of 2.1×10^{-3} mm.

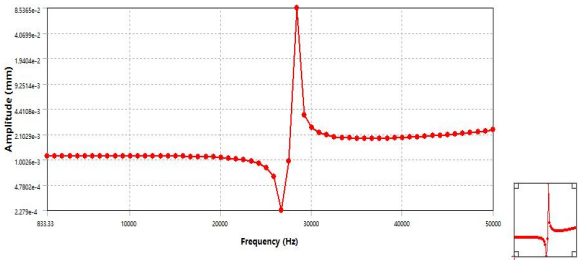

Figure 19. Rolling Bearing Amplitude Curve in the Z Direction

5. Conclusion

(1) Through free modal analysis of the deep groove ball bearing SKF6180, it was found that the growth rate of the lower-order natural frequencies of the free modal is relatively slow, while the growth rate of the higher-order free modal is faster.

(2) By conducting modal analysis of two types of constraints on rolling bearings, the modal characteristics of the bearings under different constraint types were obtained. Under

constrained conditions, the vibration modes of rolling bearings are mostly characterized by deformation from tilting and skewing of either the inner or outer ring to inward concave and twisted deformation.

(3) When the natural frequency of a structure's certain order is close to the forced vibration response frequency, mechanical resonance easily occurs, affecting structural stability. When the outer ring is constrained and the inner ring is subjected to sinusoidal excitation, its maximum peak frequency is close to the first-order natural frequency. This resonance zone should be avoided to prevent its impact on bearing vibrations by increasing system damping and enhancing structural stiffness.

Acknowledgments

This work was supported by the Scientific Research Projects of Zhoukou Normal University (KNUD2019067 and ZKNUB2201807).

References

[1] Liu J, Shao Y M. Overview of dynamic modelling and analysis of rolling element bearings with localized and distributed faults [J]. Nonlinear Dynamics, 2018, 93(4): 1765-1798.

[2] Patel S, Shah U, Khatri B, et al. Research progress on bearing fault diagnosis with localized defects and distributed defects for rolling element bearings [J]. Noise& Vibration Worldwide, 2022, 53(7 8): 352 365.

[3] He D, Yang Y, Xu H Y, et al. Dynamic analysis of rolling bearings with roller spalling defects based on explicit finite element method and experiment [J]. Journal of Nonlinear Mathematical Physics, 2022, 29(2): 219-243.

[4] Jiang Y C, Huang W T, Wang W J, et al. Acomplete dynamics model of defective bearings considering the three-dimensional defect area and the spherical cage pocket [J]. Mechanical Systems and Signal Processing, 2023, 185:109743.

[5] Cao H R, Su S M, Jing X, et al. Vibration mechanism analysis for cylindrical roller bearings with single/multi defects and compound faults [J]. Mechanical Systems and Signal Processing, 2020, 144: 106903.

[6] Luo M L, André H, Guo Y, et al. Analysis of contact behaviours and vibrations in a defective deep groove ball bearing [J]. Journal of Sound and Vibration, 2024, 570:118104.

[7] Ma H, Li H F, Yu K, et al. Dynamic modeling and vibration analysis of rolling bearings with local fault [J]. Journal of Northeastern University (Natural Science), 2020, 41(3): 343-348. (in Chinese)

[8] Tu W B, Yuan X W, Yang J W, et al. Research on dynamic characteristics of rolling bearing under different component fault conditions [J]. Chinese Journal of Engineering Design, 2023, 30(1): 82-92. (in Chinese)

[9] Yan H P, Lang S, Qin Z Y. Simulation analysis of vibration characteristics of hybrid ceramic ball bearings [J]. Machine Tool & Hydraulics, 2023, 51(13): 172-177. (in Chinese)

[10] Wang X J. Vibration response mechanism of high-speed bearing fault based on explicit dynamics [J]. Plant Maintenance Engineering, 2021(10): 67-69.(in Chinese)

[11] Li L, Wang Y L, Yang Z J. Transient dynamics and modal analysis of rocker shell of shearer [J]. Industry and Mine Automation, 2018, 44 (06): 86-89. (in Chinese)

[12] Li J Y, Wang Y L, Yang Z J. Fatigue and modal analysis of guided sliding boots of shearer [J]. Industry and Mine Automation, 2017, 43 (11): 54-57.(in Chinese)

[13] Zhang G W, Hou P P, Li J Q, Ma J Q. Study on longitudinal vibration characteristics of bha with rotary guided drilling tool [J]. Coal Mine Chinery, 2019, 40 (11): 46-49. (in Chinese)

[14] Wang D S, Chen X J, Shen D L. Analysis of modal and vibration response of gearbox box based on ANSYS workbench [J]. Coal Mine Chinery, 2020, 41(07): 69-72.(in Chinese)

